Ships and Offshore Structures

ISSN: 1744-5302 (Print) 1754-212X (Online) Journal homepage: www.tandfonline.com/journals/tsos20

Investigating the effects of weather condition uncertainties on the required propulsion power of a cruise ship

Kumars Mahmoodi, Jari Böling , Abolhassan Razminia & Roberto Vettor

To cite this article: Kumars Mahmoodi, Jari Böling , Abolhassan Razminia & Roberto Vettor (19 Aug 2025): Investigating the effects of weather condition uncertainties on the required propulsion power of a cruise ship, Ships and Offshore Structures, DOI: 10.1080/17445302.2025.2545909

To link to this article: https://doi.org/10.1080/17445302.2025.2545909

Published online: 19 Aug 2025.

SHIPS AND OFFSHORE STRUCTURES
https://doi.org/10.1080/17445302.2025.2545909

Taylor & Francis
Taylor & Francis Group

Investigating the effects of weather condition uncertainties on the required propulsion power of a cruise ship

Kumars Mahmoodi [a], Jari Böling [a,b], Abolhassan Razminia [c] and Roberto Vettor [d]

[a]Faculty of Natural Sciences and Engineering, Åbo Akademi University, Turku, Finland; [b]Automation, Mechanical and Materials Engineering, University of Turku, Turku, Finland; [c]Department of Electrical Engineering, Faculty of Intelligent Systems Engineering and Data Science, Persian Gulf University, Bushehr, Iran; [d]Napa Ltd., Helsinki, Finland

ABSTRACT

This study investigates the effects of weather condition uncertainties on the propulsion power performance of a cruise ship as a case study along a specific route. Different spatio-temporal ensemble marine weather condition parameters along the given route are adopted to estimate the uncertainties associated with the required propulsion power of the selected ship. First, based on the collected performance data of the considered ship, a feed-forward fully connected artificial neural network (FFNN) is adopted to map the complex relationships between the input data of the weather conditions and the corresponding output propulsion power data. Then, the created FFNN model is fed with all ensemble weather condition members for each grid point of the route to estimate the propulsion power uncertainties. The uncertainties are described using different statistical measures, including standard deviation, box plots, histograms, kernel density estimation, and confidence intervals. Diverse weather data sets are used to quantify the uncertainties by employing the bootstrapping method. The results showed that the weather parameters' uncertainties have considerable effects on the ship's propulsion power, leading to fluctuations in performance and efficiency. These uncertainties can cause variations in fuel consumption, which affects the overall operational costs and environmental impact of the vessel.

ARTICLE HISTORY
Received 19 March 2025
Accepted 4 August 2025

KEYWORDS
Uncertainty analysis; weather condition ensembles; ship propulsion system; cruise ship; feed-forward neural network; ERA5 data set

1. Introduction

Weather conditions, such as wind speed, wave height, and ocean currents, can significantly impact the performance of propulsion systems, fuel consumption, passenger comfort, weather routing, and the overall optimization of vessel operation and efficiency (Zheng et al. 2021; Bondarev and Greiner 2025). The influence of weather conditions on ship fuel consumption is not merely a matter of operational efficiency but a crucial aspect of addressing two pressing global concerns: carbon footprint and climate change issues. Favorable weather conditions can lead to smoother sailing and reduced fuel consumption, while unfavorable and harsh conditions can increase resistance and fuel consumption. Since many negative climate changes have occurred in the last century due to human activities, especially in the shipping industry, optimizing ship routes, speeds, and fuel efficiency in response to varying weather patterns becomes paramount. By adopting accurate weather-informed strategies and technologies, the shipping industry can reduce its carbon footprint, diminish environmental impacts, and play a vital role in transitioning towards a more sustainable and eco-friendly future.

Accurate measurement and estimation of weather parameters depend on a combination of ground, ocean, and satellite-based instruments, complemented by advanced numerical weather prediction models. Despite their complexity, these systems are inherently limited by the dynamic and chaotic nature of the atmosphere, technological constraints, and modeling assumptions (Dickson et al. 2019; Mahmoodi et al. 2021). As illustrated in Figure 1, uncertainties in weather estimation arise from various sources, including atmospheric variability, measurement errors, missing or incomplete data, and simplifications in numerical models such as coarse spatial resolution and imprecise boundary conditions (Ksciuk et al. 2023). These uncertainties can significantly affect ship operations, particularly propulsion power performance and fuel consumption. For instance, overestimating adverse weather may cause a ship to operate more cautiously

CONTACT Kumars Mahmoodi kumars.mahmoodi@abo.fi Faculty of Natural Sciences and Engineering, Åbo Akademi University, Turku, Finland

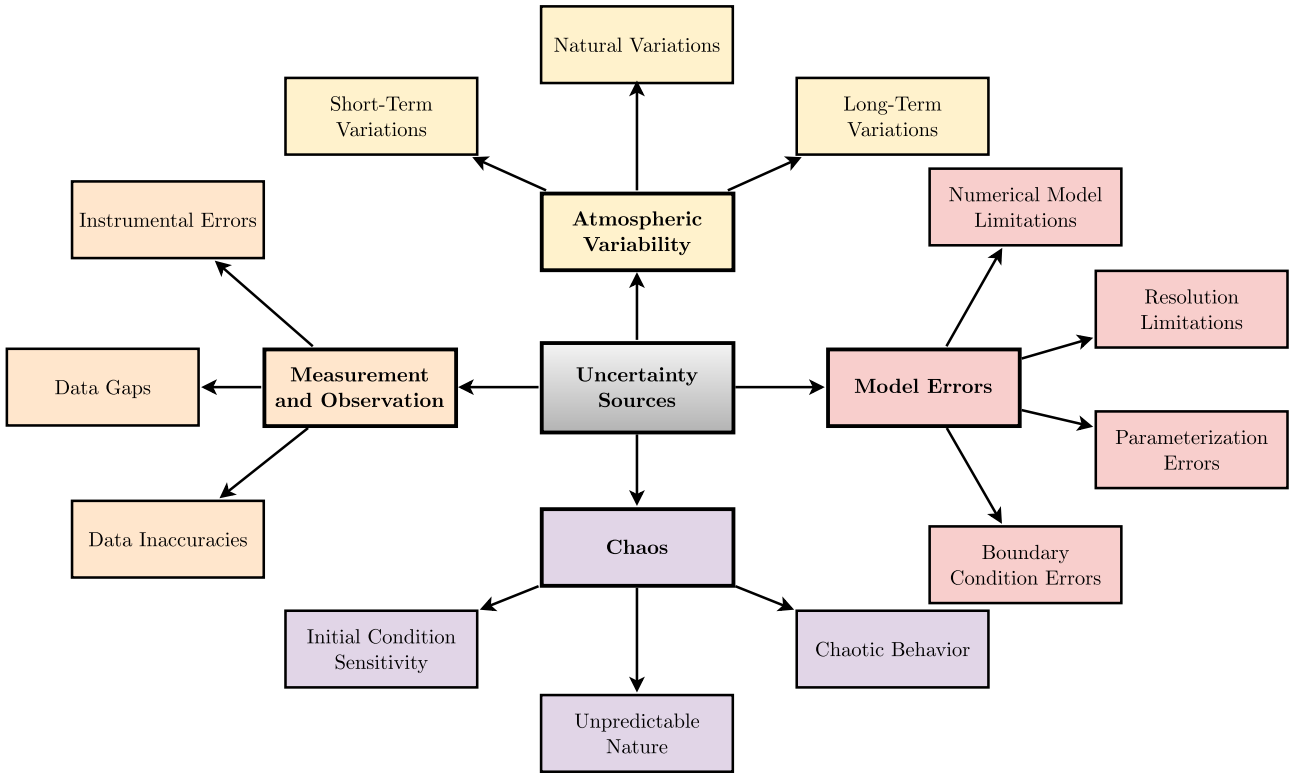

Figure 1. The primary sources of uncertainties in weather estimation. (This figure is available in colour online).

than necessary, increasing fuel use, while underestimating it may expose the vessel to unsafe conditions and inefficiencies due to reactive operational changes (Ksciuk et al. 2023; Lagemann et al. 2023). Such fluctuations in decision-making and frequent engine power adjustments degrade overall fuel efficiency and contribute to increased operational costs.

Uncertainty in weather estimation can lead to a range of negative effects on a ship's propulsion power performance and fuel consumption. These effects are often related to suboptimal operational decisions, increased engine wear, safety concerns, and the overall inefficiency of the ship's operation (Ksciuk et al. 2023; Lagemann et al. 2023). Suppose weather conditions are overestimated, for example, expecting stronger headwinds than what occurs. In this case, a ship may unnecessarily reduce its speed or increase engine power, resulting in higher fuel consumption than necessary. Conversely, if weather conditions are underestimated, a vessel may not take precautions or alter its course appropriately in the face of adverse conditions. This can lead to increased fuel consumption due to inefficient operation and the need for corrections when conditions worsen. As another example, uncertain weather conditions can lead to frequent changes in engine power and operational adjustments, which can result in inefficient engine operation. Running engines at varying power levels can reduce overall fuel efficiency.

Various research has been done on quantifying weather conditions uncertainties and their effects on ship performance and efficiency, route planning, speed profile optimization, and other related fields. The study Taskar and Andersen (2020) assessed the benefits of speed reduction for various ship types using voyage simulations, highlighting the impact of weather conditions and proposing a method to include these in shipping models. The study found that assuming a cubic relationship between speed and power can lead to significant errors in estimating fuel consumption. Study Dickson et al. (2019) presented a methodology to assess the impact of numerical errors and uncertainties of the predicted performance values made by a weather routing algorithm. It evaluated the numerical error of the routing algorithm by optimizing paths using various environmental discretizations, offering a means to quantify the significance of these errors and uncertainties in the predictive outputs. The research Ksciuk et al. (2023) offered a holistic view of uncertainties in maritime ship routing and scheduling, compares various methods, provides insights into the industry's current state, and emphasizes critical research gaps. Ensemble weather forecasts were used in Vettor et al. (2021) and Vettor and Soares (2022) to estimate the

uncertainties associated with ship fuel consumption along a specific route. Research Esmailian et al. (2022) presented a two-step approach for the efficient design of ships operating in different sea conditions while accounting for both weather and modeling uncertainties for a general cargo ship.

The study Kuroda and Sugimoto (2022) explored how variations in ship performance in real sea conditions are influenced by the routes they operate on. It specifically examined how differences in weather conditions on these routes impact the assessment of a ship's performance in actual sea conditions. Research Sui et al. (2022) investigated the operational safety of a low-powered ocean-going cargo ship in adverse sea conditions, particularly focusing on ship propulsion and maneuvering, including dynamic engine behavior when navigating through heavy weather and making head-on turns into the waves. An optimal model introduced in Li et al. (2022) for liner ship routing and scheduling, expressed as mixed integer linear programming, focused on addressing schedule-sensitive demand and late-arrival penalties. Additionally, the study presented two robust optimization versions of the deterministic ship routing and scheduling model. These robust models were designed to provide solutions under uncertain weather and ocean conditions along the Northern Sea Route. The study Luo et al. (2023) developed two methods for combining meteorological data with ship noon reports to improve the accuracy of weather information for ship speed optimization. It found that applying ensemble weather forecasts for speed optimization can significantly reduce ship fuel consumption and greenhouse gas emissions compared to deterministic forecasts.

A semi-empirical framework designed for estimating added resistance in diverse wave conditions, with a particular focus on incorporating uncertainty quantification was explored in Mittendorf et al. (2022). The calibration of the formula's parameter vector was accomplished through the use of particle swarm optimization and informed by a comprehensive database of model test results. An adaptive strategy was developed in Mason et al. (2023) to quantify stochastic uncertainty for impact reduction of forecasting uncertainties of weather routing with wind propulsion. Uncertainties of weather data were reflected employing ensemble weather forecasts for route optimization using evolutionary multi-objective weather routing strategy (Szlapczynski et al. 2023). Study Wang et al. (2023) introduced an approach for assessing collision probability among multiple ships. It employed a deep learning multi-model integration method to predict uncertain ship trajectories, enabling the quantification of time-varying stochasticity in ship motion.

Artificial neural networks (ANNs) have been increasingly applied in the maritime domain for tasks such as predicting fuel consumption, modeling ship performance, and supporting decision-making in weather routing. Several studies have demonstrated the effectiveness of ANNs in capturing complex nonlinear relationships between environmental conditions and ship responses. ANNs are being utilized for modeling, prediction, optimization, and decision-making in various ship processes (Portillo Juan and Negro Valdecantos 2022; Assani et al. 2023; Hummel et al. 2024; Imran et al. 2024; Luo et al. 2025; Zhang et al. 2025; Liu and Yuen 2025). However, most of these works have focused on deterministic modeling without adequately addressing the inherent uncertainties in weather conditions. Only a limited number of studies have explored how ensemble weather forecasts can be integrated into ANN-based frameworks to quantify the variability in ship propulsion or energy requirements. This gap highlights the need for advanced modeling techniques that not only predict ship performance but also incorporate uncertainty quantification.

The ship's propulsion system plays a crucial role in the overall operation of a vessel, impacting power generation and fuel consumption significantly (Mahmoodi et al. 2018). In general, it is the most significant contributor to fuel consumption during the voyage in the sea. The primary role of the propulsion system is to generate the necessary thrust to move the ship through the water (Mahmoodi et al. 2019a). The propulsion-generated thrust is the driving force that enables the ship to overcome water resistance and move in the desired direction. Therefore, marine weather conditions such as wind and wave patterns significantly and directly affect the ship's propulsion power performance and fuel consumption (Vettor and Soares 2022; Sui et al. 2022). Hence, the uncertainties in the estimation of the weather parameters directly affect the ship's propulsion power.

The main purpose of this study is to provide a more comprehensive understanding of how different weather scenarios can affect the ship's propulsion power performance. Assessing the range of potential outcomes under various weather conditions is possible by incorporating uncertainty estimations. For this purpose, historical ensemble weather data of the case study route are adopted to estimate the uncertainties associated with marine weather conditions. The considered strategy involves iterating feeding the case study ship propulsion power prediction model for each member of the weather parameter ensemble by employing a bootstrapping strategy. Therefore, a separate output will be obtained for each possible member of an ensemble. Various ship propulsion performance data in different weather situations are collected to build a model for predicting

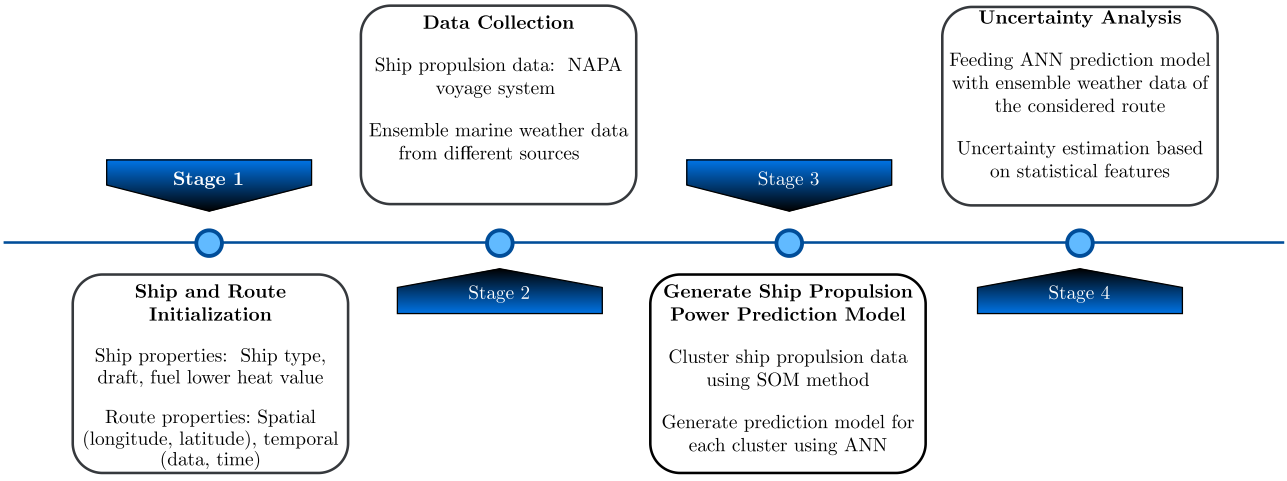

Figure 2. Proposed strategy to ship propulsion power performance uncertainty estimation. (This figure is available in colour online).

the ship's propulsion power. The feed-forward, fully connected regression neural network is adopted to map the different marine weather parameters to the output propulsion power. Due to the large volume of collected data and, on the other hand to create more accurate and effective predictive models, the Self-Organizing Map (SOM) algorithm is applied to cluster the available data into some groups with similar features. Hence, a separate FFNN model is fitted for each cluster, resulting in more suitable and accurate prediction models. Then, various statistical measures are employed to represent uncertainties. In summary, the proposed strategy to estimate the uncertainties associated with the ship propulsion power performance due to the weather parameters is illustrated in Figure 2.

The primary contribution of this study lies in the integration of spatio-temporal ensemble marine weather data with a data-driven modeling approach to evaluate the uncertainty in a cruise ship's propulsion power requirements. Unlike traditional deterministic methods, this work leverages ensemble forecasts from ECMWF ERA5 to capture a realistic range of possible weather conditions along a specific route. A feed-forward neural network model is developed and used to simulate propulsion power under each ensemble scenario, enabling a probabilistic assessment of performance. Furthermore, the study employs multiple statistical metrics–including confidence intervals, standard deviation, box plots, and kernel density estimation–to quantify and visualize the effects of weather uncertainty. This approach not only provides a more robust understanding of power performance variability but also lays the groundwork for uncertainty-aware ship energy management and routing strategies. To the best of the authors' knowledge, this is among the first studies to conduct such a detailed uncertainty analysis using ensemble data and machine learning in the maritime context.

This paper is organized as follows. The case studies of the ship and route are outlined in Section 2. Marine weather and ship propulsion power performance data sets and their sources are introduced in Section 3. In Section 4, a brief introduction of the employed methods for clustering and prediction is explored. The results and analysis of the proposed strategy are given in Section 5. Conclusions are drawn in Section 6.

2. Ship and route case studies

The first stage of the proposed methodology involves the initialization of ship and route properties. The considered ship in this study is a medium sized cruise ship. Some details of this ship are shown in Table 1. Moreover, the considered case study ship route during a month voyage (21-July-2024 to 20-August-2024) in the Atlantic Ocean is shown in Figure 3. In general, 498 points have been selected from this route with

Table 1. Specifications of the considered case study cruise ship.

Parameter	Value	Unit
Year of build	2017	–
Gross tonnage	99,000	–
Max speed	21.7	knots
Length overall	295.3	m
Beam	42.3	m
Draught	8.2	m
Summer deadweight	7900	t
Total installed power	48,000	kW
Main engine configuration	2 × 9.6 MW Wärtsilä 8L46F 2 × 14.4 MW Wärtsilä 12V46F	–
Propulsion type	Diesel-electric	–
Propulsion arrangement	Two shafts with fixed pitch propellers	–
Thrusters	Three bow thrusters, two stern thrusters	–
Passenger capacity	2534	persons

Figure 3. Considered case study ship route during one month voyage [red line]. (This figure is available in colour online).

hourly temporal resolution. These points are selected in such a way that their data are available and the ship is moving and not in port. Moreover, the ship's draught is assumed to be constant throughout the analysis.

3. Data sets

3.1. Marine weather data

The marine and weather data of the selected points along the studied route is provided by several sources as presented in Tables 2 and 3. These data sets include a variety of parameters such as wind and swell wave heights, wind speed, and ocean currents, which are crucial for accurate navigation and safety at sea. By integrating these diverse data sources, it is possible to achieve a comprehensive understanding of the marine environment, enhancing the accuracy of the predictions and uncertainty analysis. Depending on the specific model, some data have been interpolated to provide hourly values, while certain weather variables may not be available across all models. The data from Meteo-France MFWAM and SMOC Currents offer high spatial resolution, making them ideal for detailed regional analysis. ECMWF WAM and NCEP GFS Wave provide global coverage with frequent updates, ensuring up-to-date information for long-distance routes. ERA5-Ocean offers comprehensive historical data with a slight delay, useful for retrospective studies and model validation. It includes a short-term uncertainty estimate generated by a 10-member EDA system (Isaksen et al. 2010) for each weather parameter.

The list of collected marine weather parameters is shown in Table 4. The speed (SCS) and direction (SCD) of the sea current are obtained from Meteo-France SMOC Currents data set for the studied route. As an example, Figure 4 illustrates the collected ensemble wind speed, significant height of wind and swell waves, and their periods for the considered route points. In this figure, the solid line and the shaded area around

Table 2. Data sources of considered marine variables (Open-Meteo 2024; Deutscher Wetterdienst 2024).

Data Set	Region	Spatial Resolution	Temporal Resolution	Update Frequency
MeteoFrance MFWAM	Global	0.08° (8 km)	3-Hourly	Every 12 h
MeteoFrance SMOC Currents	Global	0.08° (8 km)	Hourly	Every 24 h
ECMWF WAM	Global	0.25° (25 km)	3-Hourly	Every 6 h
NCEP GFS Wave	Global	0.25° (25 km)	Hourly	Every 6 h
DWD GWAM	Europe	0.05° (5 km)	Hourly	Every 12 h
DWD EWAM	Global	0.25° (25 km)	Hourly	Every 12 h
ERA5-Ocean	Global	0.5° (50 km)	Hourly	Every 24 h with 5 days delay

Table 3. Considered weather models and their features (Open-Meteo 2024; Deutscher Wetterdienst 2024).

Weather Model	National Weather Provider	Resolution	Forecast Length	Update Frequency
ICON	Deutscher Wetterdienst (DWD)	2–11 km	7.5 days	Every 3 h
GFS & HRRR	NOAA	3–25 km	16 days	Every hour
ARPEGE & AROME	Météo-France	1–25 km	4 days	Every hour
IFS & AIFS	ECMWF	25 km	7 days	Every 6 h
MSM & GSM	JMA	5 – 55 km	11 days	Every 3 h
MET Nordic	MET Norway	1 km	2.5 days	Every hour
HARMONIE	KNMI	2 km	2.5 days	Every hour
HARMONIE	DMI	2 km	2.5 days	Every 3 hours
GEM	Canadian Weather Service	2.5 km	10 days	Every 6 h
GFS GRAPES	China Meteorological Administration (CMA)	15 km	10 days	Every 6 h
ACCESS-G	Australian Bureau of Meteorology (BOM)	15 km	10 days	Every 6 h

Table 4. The details of the collected marine weather and ship data from the NAPA Voyage system (NAPA 2023).

Category	Parameter	Abbreviation	Range	Unit
Ship	Draught	–	8.2	m
	Fuel lower heat value	–	41600	kJ. kg^{-1}
	Speed over ground	SOG	3–11	m. s^{-1}
	Course over ground	COG	0–360	degrees
	Propulsion power	POW	272.8–45201	kW
Weather	Wind speed	WSP	0–15	m. s^{-1}
	Wind direction	WID	0–360	degrees
	Significant height of wind waves	SWW	0.5–3.5	m
	Wind waves zero crossing mean period	WWP	1–10	s
	Wind waves mean direction	WWD	0–360	degrees
	Swell significant wave height	SWH	0–1	m
	Swell mean period	SMP	1–15	s
	Swell mean direction	SMD	0–360	degrees
	Sea current speed	SCS	0–1.5	m. s^{-1}
	Sea current direction	SCD	0–360	degrees
Route	Water depth	WAD	50–500	m

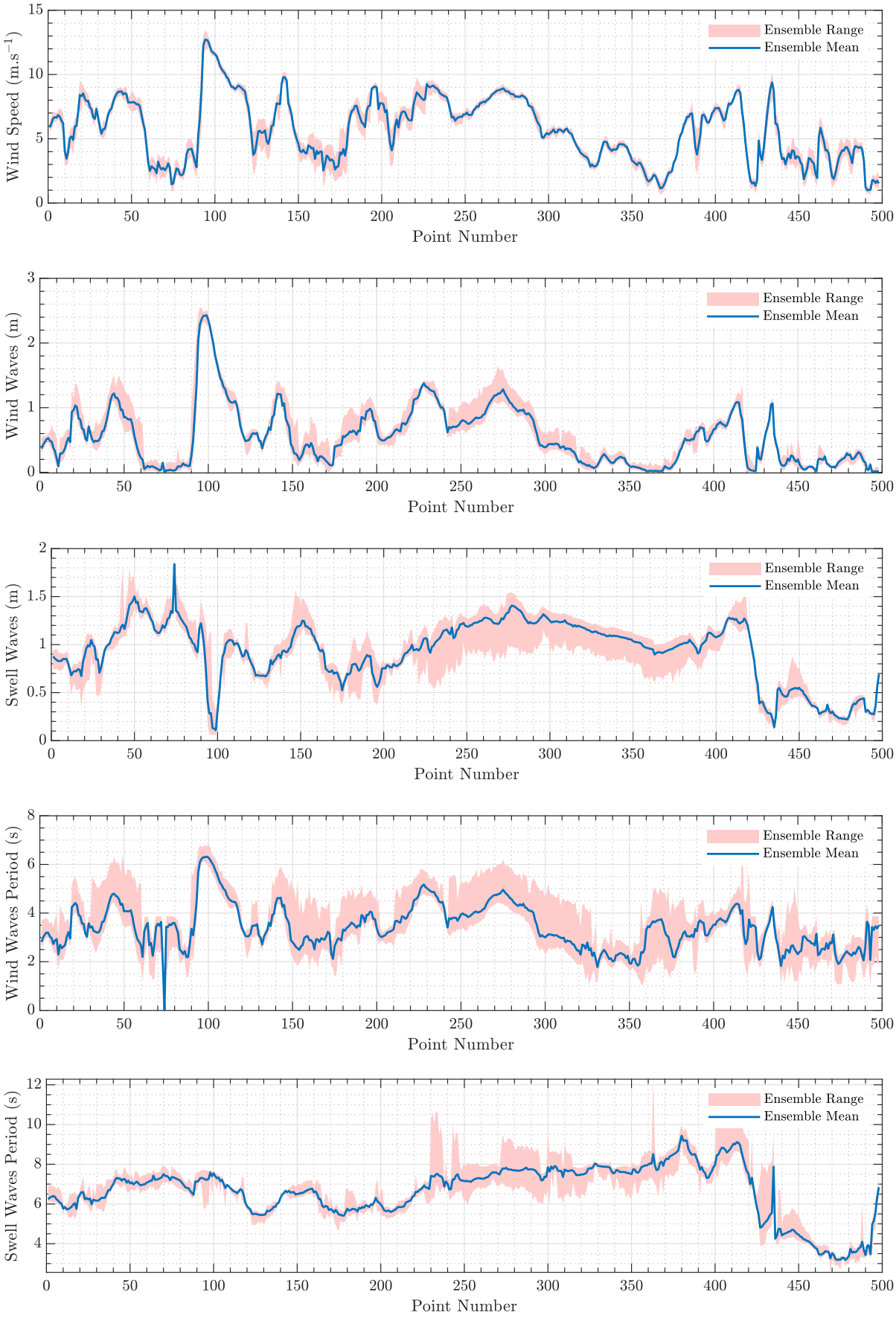

Figure 4. The ensemble marine weather parameters for the considered route points. (This figure is available in colour online).

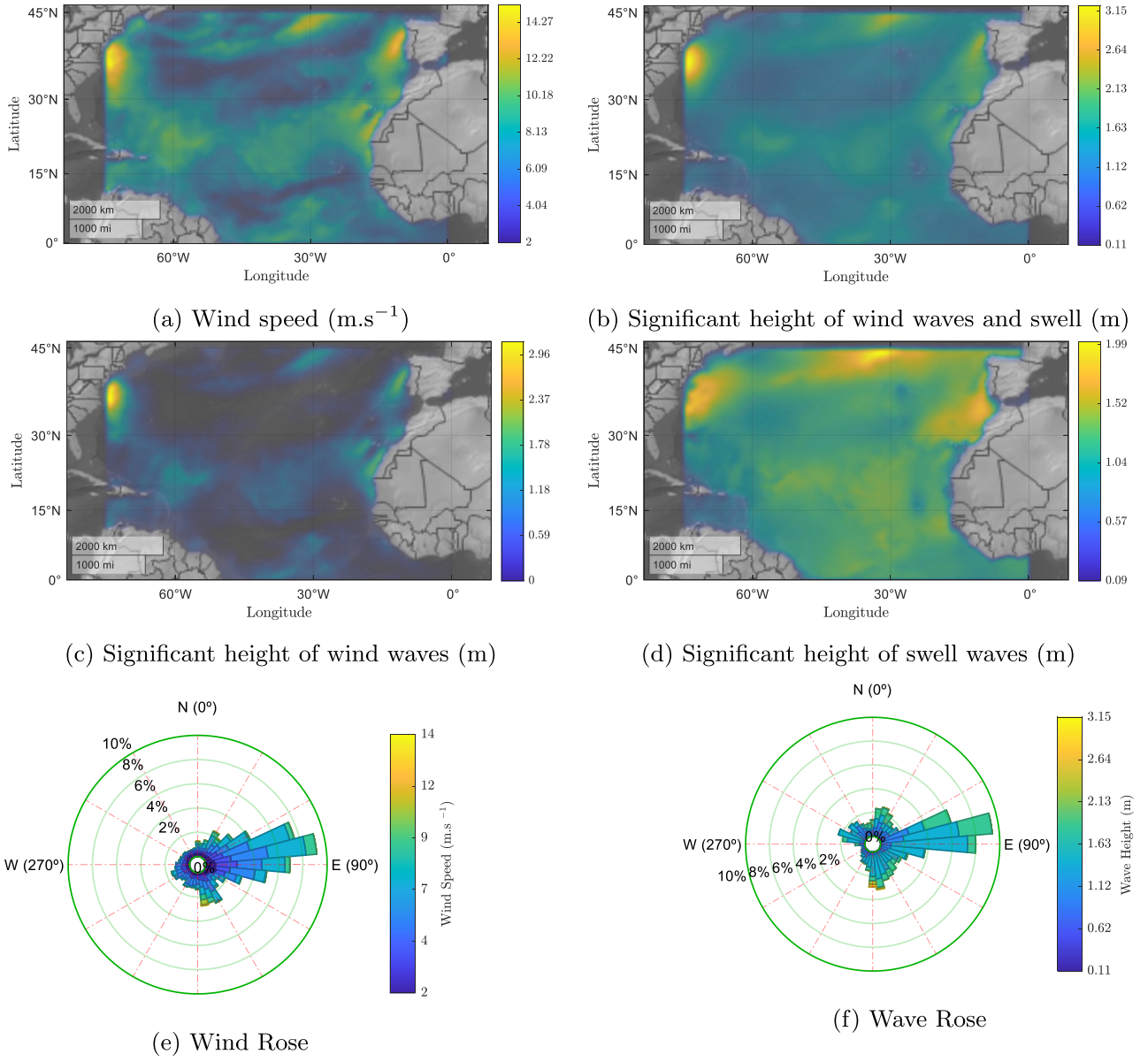

(a) Wind speed (m.s^{-1})

(b) Significant height of wind waves and swell (m)

(c) Significant height of wind waves (m)

(d) Significant height of swell waves (m)

(e) Wind Rose

(f) Wave Rose

Figure 5. The spatio-temporal variations of the considered marine weather parameters across the studied area at 2024-08-09T10:00:00Z based on ERA5 data set. (a) Wind speed (m.s^{-1}). (b) Significant height of wind waves and swell (m). (c) Significant height of wind waves (m). (d) Significant height of swell waves (m). (e) Wind Rose and (f) Wave Rose. (This figure is available in colour online).

it represent the mean and range of ensemble members, respectively. Moreover, the spatio-temporal variations of wind speed, wind and swell significant wave heights, wind and wave roses across the studied area at 2024-08-09T10:00:00Z are shown in Figure 5 based on ERA5 data set. The open-source Matlab code Pereira (2024) is used to plot the wind and wave roses.

3.2. Ship propulsion power performance data

The ship propulsion data is collected from NAPA voyage system (NAPA 2023). As mentioned earlier, these data have been used to build the FFNN predictive model of the ship propulsion power performance model. The FFNN model maps the marine weather data and ship movement parameters to the needed ship propulsion power. Table 4 shows the details of the collected marine weather and ship data. A total of 50,000 date records of ship performance under various weather conditions have been collected in such a way that they can provide a satisfactory description of the behavior of the system in different conditions.

4. Methods

4.1. Self-Organizing map neural network

As previously stated, to obtain more accurate FFNN predictive models for the ship propulsion, the data are

clustered and a separate model is developed for each cluster. In this research, the SOM neural network is used to cluster the data by similarity. A SOM network, also known as Kohonen network (Kohonen 2001), is a type of ANN designed to perform unsupervised learning that can be used for various purposes, including data clustering, dimension reduction, and feature mapping. It is capable of handling nonlinear and high-dimensional data, which can prove challenging for conventional clustering approaches such as *k*-means (Mahmoodi and Nowruzi 2022).

The SOM network is known for preserving the topological relationships within data, enabling it to uncover complex data structures and patterns effectively. It means that similar input data points will be mapped to nearby locations on the SOM grid-like structure, typically two-dimensional regular spacing in a hexagonal or rectangular grid. Each node in the grid is called a neuron, and it is associated with a weight vector of the same dimension as the input data. The number of neurons in the grid can be determined based on the desired number of clusters or through experimentation. The neurons in a SOM network layer are organized in physical positions based on a predefined topology function.

SOM employs competitive learning and a neighborhood function to preserve the topological characteristics of the input data, resulting in a topologically ordered representation in the grid of neurons. In competitive learning, each input data point competes to determine which neuron in the grid it is most similar to. The neuron with the weight vector most similar to the input data is called the winner or activated neuron. Instead of updating only the winning neuron i^*, the update extends to all neurons within a specified neighborhood, $N_{i^*}(d)$, of the winning neuron, utilizing the Kohonen rule. In particular, all neurons $i \in N_{i^*}(d)$ are adjusted as follows (The MathWorks, Inc. 2024):

$$\mathbf{w}_i(q) = \mathbf{w}_i(q-1) + \alpha\big(\mathbf{p}(q) - \mathbf{w}_i(q-1)\big) \qquad (1)$$

where $\mathbf{w}_i(q)$ is the weight vector of the neuron i at step q and α is the learning rate which determines the magnitude of the adjustment. The learning rate decreases over time to ensure that the map converges to a stable state gradually. $\mathbf{p}(q)$ is the input vector at step q which represents the current input or data sample being presented to the SOM network.

The winning neuron and its neighboring neurons adjust their weight vectors to become more similar to the input data vector $\mathbf{p}$, a process called adaptation or learning. This is done iteratively over the entire dataset. The similarity is often calculated using measures like Euclidean distance. The neighborhood function is used to determine which neurons are affected by the adaptation process. The neighborhood $N_{i^*}(d)$ comprises the indices of all neurons located within a distance d from the winning neuron i^*:

$$N_i(d) = \{j \mid d_{ij} \le d\} \qquad (2)$$

Initially, the neighborhood area is relatively large and covers a larger part of the map. As training progresses, the neighborhood area becomes smaller and the adaptation process focuses on a smaller part around the best-matching neuron. The number of training iterations and the learning rate are important parameters that need to be tuned based on the specific clustering task and dataset. Once the SOM has been trained, the weight vectors of the neurons represent the cluster prototypes. Each neuron corresponds to a cluster, and the input data points are assigned to the nearest neuron. It is possible to visualize the clusters and their relationships in a 2D space by mapping the weight vectors onto a two-dimensional grid.

4.2. Feed-forward artificial neural network

As mentioned before, a feed-forward fully connected ANN method is utilized in this study to model the complex relation between the ship and weather parameters to the ship propulsion power output. It is a type of artificial neural network architecture that consists of layers of interconnected neurons or nodes (Mahmoodi et al. 2020; El-shenawy et al. 2025). A general schematic of a multi-layer (in this case three-layer) neural network architecture is illustrated in Figure 6. In this figure, a superscript number i is added to the variables of interest to indicate which layer it belongs to. In the considered FFNN structure, information flows from the input through one or more hidden layers to the output layer. The inputs to each subsequent layer are derived from the outputs of the preceding layer. Each hidden and output layer has a weight matrix W^i, a bias vector $\mathbf{b}^i$, and an output vector $\mathbf{h}^i$. The input consists of R nodes (neurons) that represent the input features or variables for each input vector $\mathbf{p}$ of the data set. Each node in the input corresponds to one feature. One or more hidden layers, each of which with S^i number of hidden neurons, can be placed between the input and the output layer. Each node in a hidden layer is fully connected to every node in the previous and subsequent layers that information passes through these connections (Mahmoodi et al. 2019b; Wu et al. 2025). The number of output layer nodes is equal to the number of output variables. Here, it is assumed that the third layer's output, $\mathbf{h}^3$, is the network output.

In a feed-forward network, the output of each node h_j^i ($j = 1 : S^i$) is provided by its inputs, weights, biases, and

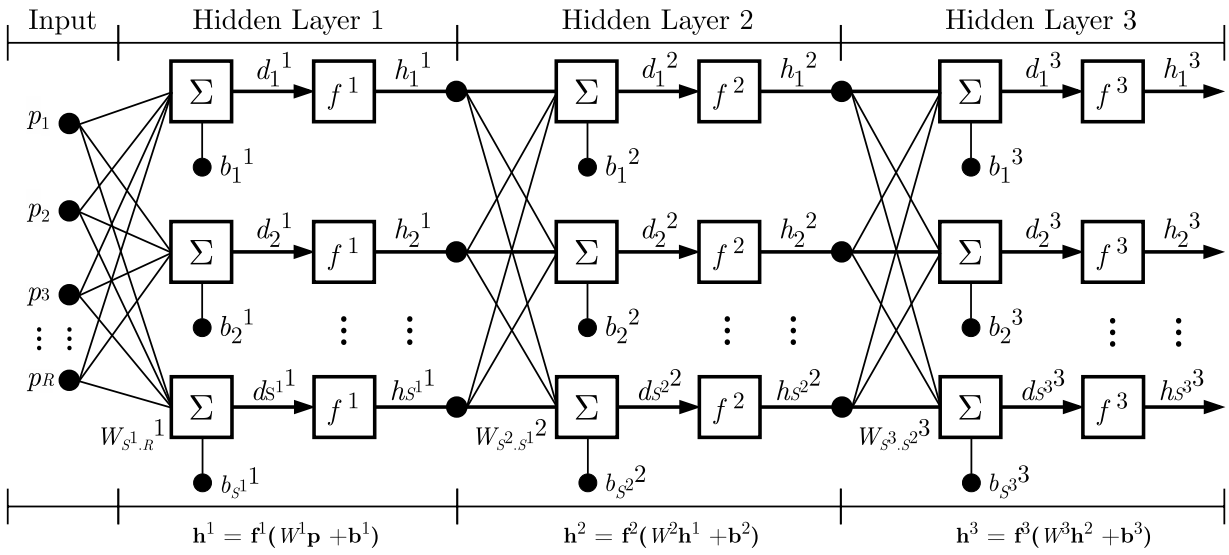

Figure 6. A general schematic of a multi-layer neural network architecture [in this case three-layer].

activation function f using a process called forward propagation. During the forward propagation process, data is passed forward through the network layer by layer to produce a prediction or output. All connections between nodes in adjacent layers are associated with weights W^i that determine the strength of the connection between them (Mahmoodi and Nowruzi 2022). In addition, nodes can be associated with biases $\mathbf{b}^i$ that allow the network to account for variations in the data that are not solely explained by the weights and the input data. Bias terms are usually associated with neurons in the hidden layers and the output layer. These bias terms in the hidden layers help the network for more flexibility in modeling complex relationships in the data. The bias terms in the output layer contribute to the final predictions of the network. Activation functions f^i are mathematical functions applied to the summation of weighted inputs and biases of a node in an FFNN structure that introduces non-linearity into the network. Common activation functions include sigmoid, hyperbolic tangent (tanh), and rectified linear unit (ReLU) (The MathWorks, Inc. 2024).

Weights W^i and biases $\mathbf{b}^i$ are treated as learnable parameters during the training process to make accurate predictions by minimizing loss function based on their optimal values (Mahmoodi et al. 2022). Backpropagation is the process by which the network adjusts its weights and biases based on the error or loss between the predicted output and the actual target values using optimization techniques like gradient descent. The learning rate parameter determines the size of these weight and bias updates. The learning process continues for a certain predefined number of iterations or until the loss converges to a satisfactory level. In the training process, the network outputs are tried to be as close as possible to the target actual values.

Weight sensitivity analysis helps in understanding which weights are more influential in the network's behavior and can provide insights into the importance of specific features or connections in the learning process. It can be used as a way to understand the importance of different input variables or features on the predictive model's output. The influence percentage of the input variable p_r on the output variable o_k, Q_{rk}, can be determined as follows (Vaghefi et al. 2020):

$$Q_{rk} = \frac{\sum_{j=1}^{S}\left(\frac{|w_{rj}|}{\sum_{r=1}^{R}|w_{rj}|}|v_{jk}|\right)}{\sum_{r=1}^{R}\left(\sum_{j=1}^{S}\left(\frac{|w_{rj}|}{\sum_{r=1}^{R}|w_{rj}|}|v_{jk}|\right)\right)} \times 100\% \quad (3)$$

where w_{rj} describes the weight between the input neuron $p_r (r = 1, 2, \ldots, R)$ and the hidden neuron m_j $(j = 1, 2, \ldots, S)$, and v_{jk} depicts the weight between the hidden neuron j and the output neuron o_k $(k = 1, 2, \ldots, L)$.

5. Results

In this section, the results of modeling and data analysis are presented. In the first step of modeling, the ship propulsion data are clustered into several similar groups by the SOM-neural network method to make more accurate FFNN predictive models for each cluster. After categorizing the ship propulsion power data into different clusters, a predictive FFNN model can be created for each cluster.

Table 5. The structure of the selected SOM neural network to cluster the ship propulsion data.

Parameter	Value
Data set	50,000 observations with 13 features
Number of layers	single competitive layer
Map size	3×3
Map topology	Hexagonal
Number of neurons	9
Training algorithm	Batch unsupervised training
Performance function	Mean Square Error (MSE)
Maximum number of epochs	1000

As previously stated, this strategy increases the prediction accuracy. Then, several statistical measures are employed to gain a comprehensive understanding of uncertainty in the ship propulsion power data. MATLAB software is used for modeling and data analysis.

5.1. Clustering of the ship propulsion power performance data

The overall ship propulsion power performance data set contains 50,000 observations, each with 13 features (see Table 4). Constants (i.e. Draught and Fuel lower heat value) are not considered in the clustering. The structure details of the selected SOM neural network with a single competitive layer are presented in Table 5. Moreover, its schematic diagram is illustrated in Figure 7. To create the SOM network, the map size is set to 3×3, this corresponds to a grid with 3 rows and 3 columns. Therefore, the total number of neurons/clusters is equal to 9. The batch unsupervised algorithm is applied to train the network and update weights and biases. Updates to weights and biases take place upon completing a full pass through the input data. Each SOM network training session begins with distinct initial weights and biases and can result in an enhanced network through subsequent retraining. Hence, the network has been trained several times and the results of the best network are presented.

The topology of the SOM network is considered to be hexagonal. Therefore, in the following figures, each of the hexagons represents a neuron. The SOM network

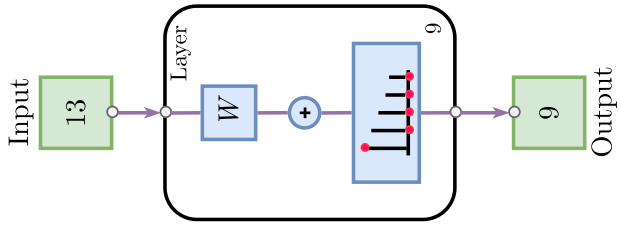

Figure 7. Schematic diagram of the selected SOM neural network with a single competitive layer. (This figure is available in colour online).

sample hits are shown in Figure 8(a). It shows the neuron locations in the topology and indicates how many data points are associated with each neuron (cluster centers). As it is clear from this figure, there are a total of 9 clusters, the largest cluster has 5909 members and the smallest one has 4970 members. Figure 8(a) shows the weight distance matrix of the created SOM network. In this figure, neurons are depicted as blue hexagons. Red lines link neighboring neurons, and the colors within the regions outlined by these lines represent the distances between neurons. Darker colors indicate larger distances, while lighter ones indicate smaller distances. Moreover, the weight plane for each feature of the considered data set is presented in Figure 9. These are graphical representations of the weights linking every input to each individual neuron (Brighter and darker colors indicate larger and smaller weights, respectively). The more similar connection patterns of features mean that they are highly correlated. According to this figure, it can generally be said that the features are not highly correlated to each other.

5.2. Generating the ship propulsion power prediction models

A feed-forward, fully connected regression neural network is trained for each created cluster from the previous subsection. Here also, the networks have been trained several times to achieve higher accuracy models, and the results of the best obtained model are presented. The general structure details of the created neural networks are presented in Table 6. To build a predictive model for each cluster, there are 13 input variables (Predictors) and one output variable (Response). It is necessary to explain that all the variables where their unit is degree are calculated relative to the COG variable. The number of observations for each model (cluster) is depicted in Figure 8(a). There are 100 outputs in the first fully connected layer and 1 output in the second fully connected layer. This number was chosen as a result of empirical testing and iterative retraining procedures. The FFNN was retrained multiple times using different random initializations and training-validation splits to ensure the robustness and consistency of its predictive performance. The architecture was selected based on the model's ability to minimize the validation error while avoiding overfitting. A ReLU activation function is used for the hidden layer. Predictors are standardized for better results. Here, k-fold cross-validation is utilized to reduce the model overfitting by evaluating the model's performance on multiple subsets (folds) of the data. It helps to reduce the impact of the randomness in the data splitting process and as a result,

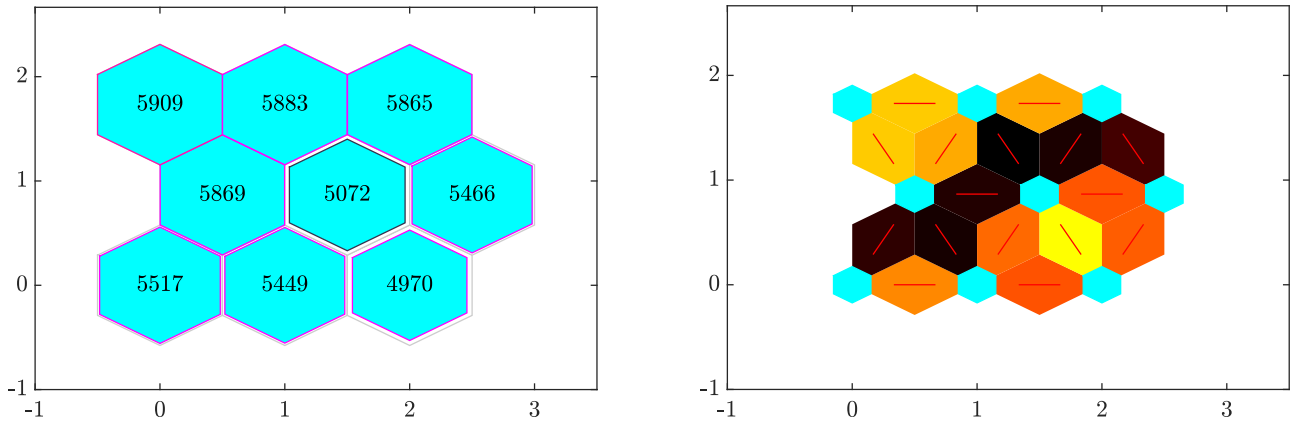

Figure 8. The sample hits and weight distance matrix of the created SOM network for the ship propulsion power performance data set. (a) Sample hits and (b) Weight distance matrix. (This figure is available in colour online).

provides a more reliable estimate of a model's performance compared to a single train-test split.

The summary of the created FFNN models for different clusters is presented in Table 7. The considered model performance criteria are Mean Absolute Error (MAE), Mean Absolute Percentage Error (MAPE), Root Mean Square Error (RMSE), Scatter Index (SI), and the square of the correlation coefficient R^2. The closer the error measures are to zero and R^2 is closer to one, it means that the models are created with higher accuracy. As it is clear from Table 7, the models have been created with acceptable accuracy. Moreover, a comparison of the observed and FFNN predicted ship propulsion power values for created clusters is shown in Figure 10. A well-performing model generates predictions that are closely distributed around the straight line. As it is evident from this figure, the concentration of data is around the straight line which means that the models are created with suitable accuracy. As an example, Figure 11 shows the outputs of the created FFNN models for new input data based on SWW, WSP, and SOG variables.

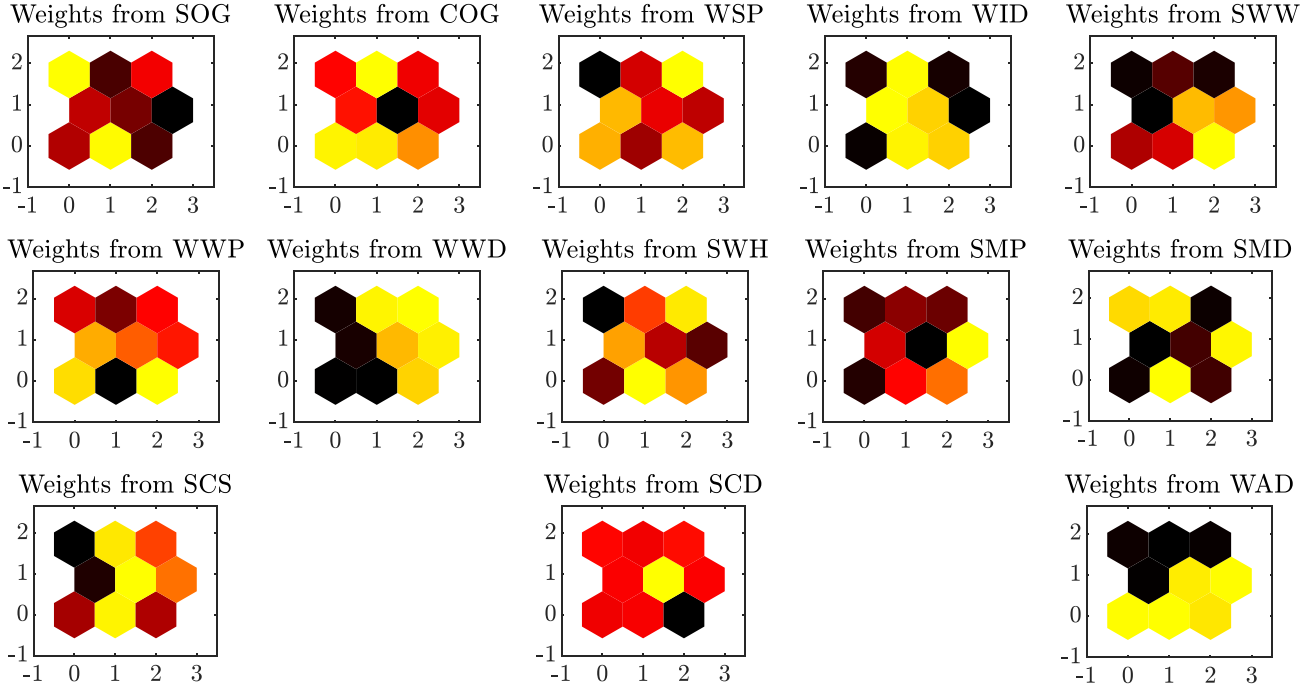

Figure 9. The weight plane of the created SOM network for each feature of the ship propulsion power performance data set (See Table 4). (This figure is available in colour online).

Table 6. The general structure details of the created FFNN models to generate ship propulsion power prediction models.

Parameter	Value
Type	Regression Neural Network
Predictors	SOG, COG, WSP, WID, SWW, WWP, WWD, SWH, SMP, SMD, SCS, SCD, WAD
Response	POW
Standardize the predictor data	True
Number of layers	Two layer
Hidden Layer size	100
Hidden layer activation function	ReLU
Output layer activation	None
Training data ratio	70% of the whole data set
Validation data ratio	15% of the whole data set
Test data ratio	15% of the whole data set
Layer weights initializer	Glorot (Glorot and Bengio 2010)
Layer biases initializer	Zeros
Update the network learnable parameters	limited memory Broyden-Fletcher-Goldfarb-Shanno quasi-Newton algorithm (LBFGS) (Nocedal and Wright 2006)
Regularization strength (Lambda)	0
Relative gradient tolerance	1e−6
Loss tolerance	1e−8
Performance function	Mean Square Error (MSE)
Maximum number of epochs	1000
Cross-validation	5-fold cross-validation

Table 8 gives insights into which input variables have the most significant impact on the network's output (ship propulsion power) for each cluster utilizing weight sensitivity analysis. It helps identify the relative importance of different input variables in predicting the output. Higher percentage values indicate higher sensitivity, suggesting that changes in those variables have a more noticeable effect on the predicted propulsion power. The values in the table represent the percentage change in the output for a 1% change in the corresponding input variable. According to the results of Table 8, in general, it can be concluded that the SOG has the highest and COG has the lowest effect on the propulsion power.

5.3. Uncertainty analysis

In this subsection, the created predictive FFNN models are fed with different ensemble weather data sources (See Subsection 3.1) of the considered points of the case study route. The bootstrapping method is used to better capture the range of possible outcomes and provide more reliable estimates of the required propulsion power. Bootstrapping is a powerful non-parametric statistical technique that can significantly enhance the accuracy of uncertainty estimation by repeatedly resampling the observed data with replacement. Number of bootstrap iterations is set to 10000 for each route point.

Table 7. The performance of the created FFNN models for the ship propulsion power data.

Clusters	MAE (kW)	MAPE (%)	RMSE (kW)	SI (%)	R^2
Cluster 1	843.6587	9.8451	1010.9512	6.9563	0.9723
Cluster 2	665.2145	7.5142	860.6410	5.7325	0.9755
Cluster 3	588.9541	6.7536	725.7425	4.9563	0.9781
Cluster 4	875.9874	9.961	1132.5656	7.1478	0.9722
Cluster 5	601.3625	7.8541	705.8416	5.2536	0.9778
Cluster 6	639.2233	7.5684	800.5203	5.8796	0.9762
Cluster 7	722.7485	9.5540	902.4789	6.5412	0.9712
Cluster 8	855.9632	9.9998	1100.1457	7.9583	0.9721
Cluster 9	821.7583	9.8536	1044.6932	6.4728	0.9742

In the first step of ship propulsion power uncertainty analysis, the cluster of each ensemble member of the studied points should be determined. Therefore, the ensemble members are fed to the created SOM network model in the Subsection 5.1. The results are depicted in the Figure 12. As it is clear in this figure, most of the ensemble member data (51%) are located in cluster 1 and then cluster 7. In the second step, the ensemble members are fed to the created FFNN models depending on which cluster they belong to. For example, if an ensemble member belongs to cluster 1, then it will be sent to the FFNN model 1 to estimate its propulsion power output.

Figure 13 shows the ensemble outputs of the FFNN models of the studied route points. It should be noted that the uncertainty range is invisible in some parts of this figure due to its small range. Also in this figure, the main plot is divided into four equal parts to show better the uncertainty ranges in the route points. According to this figure, the uncertainty range values vary significantly, from as low as 1841 kW to as high as 9653 kW. This suggests that under certain conditions, the required propulsion power can differ substantially depending on the weather and environmental factors. There are some high uncertainty values (above 9000, such as 9653 kW), which could indicate extreme weather conditions or outliers in the model's response to certain perturbations. Conversely, low uncertainty values (such as 1841 kW) may indicate stable or less sensitive scenarios where the required propulsion power is relatively predictable and does not vary much. A large portion of the uncertainty ranges for the considered points seems to fall within the range of approximately 3000 to 6000 kW. This suggests that for most scenarios, the propulsion power uncertainty is within a predictable range. The magnitude of these uncertainties highlights the potential impact of weather and sea conditions on the propulsion power. For example, if the uncertainty is 6000 kW, this suggests that for a given scenario, the required propulsion power might vary by this amount from one estimate to another. In practical terms, this variability means that in extreme conditions, the ship could need significantly more propulsion power than under calm or predictable conditions.

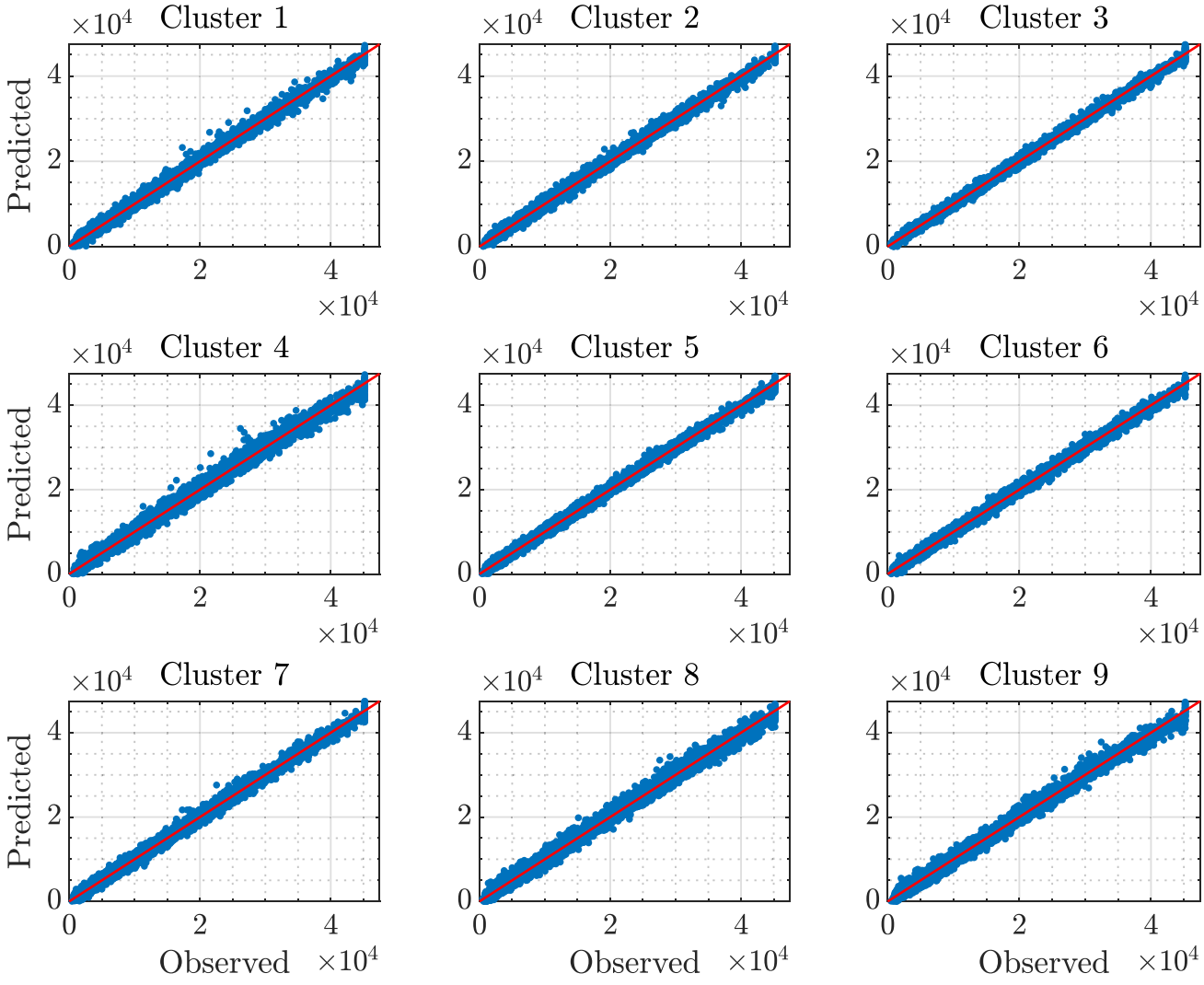

Figure 10. Comparison of the observed and FFNN predicted ship propulsion power values (in kW) for created clusters. (This figure is available in colour online).

Figure 14 shows the histogram and boxplot of the uncertainty ranges of the considered route points. A histogram and box plot of the uncertainty ranges could visually illustrate the spread and frequency of different uncertainty levels which can help to identify typical vs. extreme cases. The histogram shows a right-skewed distribution, with most values clustering around 3500 to 5500 kW. This indicates that the majority of the

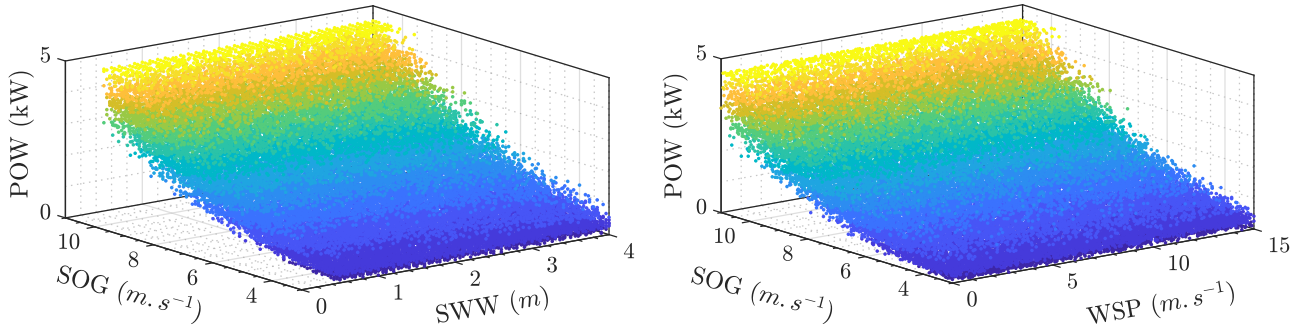

(a) POW vs. SWW and SOG. (b) POW vs. WSP and SOG.

Figure 11. The outputs of the created FFNN models for new input data based on SWW, WSP, and SOG variables. (a) POW vs. SWW and SOG and (b) POW vs. WSP and SOG. (This figure is available in colour online).

Table 8. Variable importance analysis of the created neural network models for the ship propulsion power data (Results are in %).

Parameter	Cluster 1	Cluster 2	Cluster 3	Cluster 4	Cluster 5	Cluster 6	Cluster 7	Cluster 8	Cluster 9
SOG	15.3094	13.3797	18.9224	12.3895	13.7982	14.0362	15.8575	25.3693	14.6551
COG	8.5344	8.6414	4.2216	7.9679	8.4861	8.6238	7.0352	3.6613	8.9751
WSP	8.3529	8.9366	12.6735	9.7629	9.6732	9.5023	8.6662	10.6112	6.3174
WID	9.0258	7.0295	11.2521	8.3592	6.7141	7.1347	9.2533	3.1563	7.2699
SWW	6.0345	6.7233	3.8043	7.4963	8.7990	6.1504	6.0449	3.3394	6.4759
WWP	6.9872	7.2693	9.8104	8.1158	8.9719	5.9851	6.7182	4.0242	6.5529
WWD	6.5080	4.9073	3.9024	5.6356	4.9510	6.2012	3.9436	8.3265	5.6113
SWH	6.4306	8.8760	9.2726	7.7135	7.2588	8.6479	9.4019	12.0889	7.8198
SMP	8.0557	8.3775	6.0877	8.7913	7.4177	8.3336	7.8946	4.1353	6.5393
SMD	6.4885	6.9049	2.8878	6.1317	7.4365	9.0241	6.5034	1.3991	7.6638
SCS	6.3282	5.4808	7.3791	6.3233	4.6378	4.7431	7.5243	12.8845	7.8443
SCD	4.9123	4.4016	2.3301	3.2739	3.2728	3.8322	4.2489	4.8040	7.5303
WAD	7.0324	9.0720	7.4561	8.0391	8.5828	7.7853	6.9081	6.2000	6.7450

uncertainty in propulsion power lies within this range. Although the frequency is much lower, there are points where the uncertainty in propulsion power goes above 7000 kW, with a few values approaching 10,000 kW. The median value (red line inside the box) is around 4500 kW which shows half of the propulsion power uncertainties are below this value, while the other half are higher. Moreover, the whiskers extend down to about 2000 kW on the lower end and to about 7000 kW on the upper end which shows the range of typical values. Both the histogram and box plot illustrate a predominantly moderate uncertainty range for propulsion power requirements (3500–5500 kW), but with the possibility of high-end outliers in the 7000–10,000 kW range.

The Standard Deviation (STD), Coefficient of Variation (CV), and Interquartile Range (IQR) of the route points ship propulsion ensemble members are illustrated in Figure 15. STD indicates how spread out the ensemble values are for each route point. Larger standard deviations indicate higher uncertainty in propulsion power predictions. IQR highlights how the bulk of ensemble values vary. CV is the ratio of the standard deviation to the mean. It standardizes the uncertainty relative to the average propulsion power. High CV values suggest large uncertainty relative to the mean. Here, the CV values are multiplied by 1000 to display this variable better and scale it with other parameters. Figure 16 shows the 95% confidence interval around the mean of each route point ship propulsion power members for some points of the considered route. In this figure, only a part of the points is displayed for clarity and better display of details. The vertical bar at each data point depicts the lower and upper bounds of the 95% confidence intervals. A 95% confidence interval implies that there is a 95% probability that the true propulsion power mean lies within the calculated interval. In general, the range of points' confidence levels are not significantly different from each other.

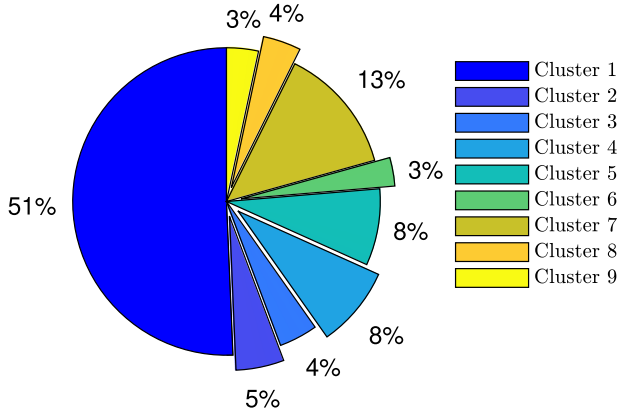

Figure 12. The belonging percentage of the route points ensemble members to the created clusters. (This figure is available in colour online).

Analyzing uncertainties in ensemble data for ship propulsion involves understanding the variability across the ensemble members and their statistical characteristics along route points. Here, 10 points of the route are arbitrarily selected for a deeper uncertainty analysis. The indices of these points are 9, 67, 82, 137, 191, 281, 309, 341, 344, and 383. Table 9 provides some measures of the central tendency, spread or variability, and distribution of the ensemble members of the ship propulsion power outputs for the considered route points. The mean represents the central tendency, while the standard deviation gives a measure of the spread or variability in the data. A larger standard deviation indicates greater variability in the data. Therefore, the low standard deviation values in this table show that the data points tend to be close to the ensemble mean. A lower CV suggests lower relative variability. As it is clear from the results of Table 9, the CV of ensemble members is small which means low variability. The skewness and kurtosis provide insights into the shape of data distribution. Positive skewness in the table indicates that the right tail of each point distribution is longer than the left tail (mean greater than the median), while

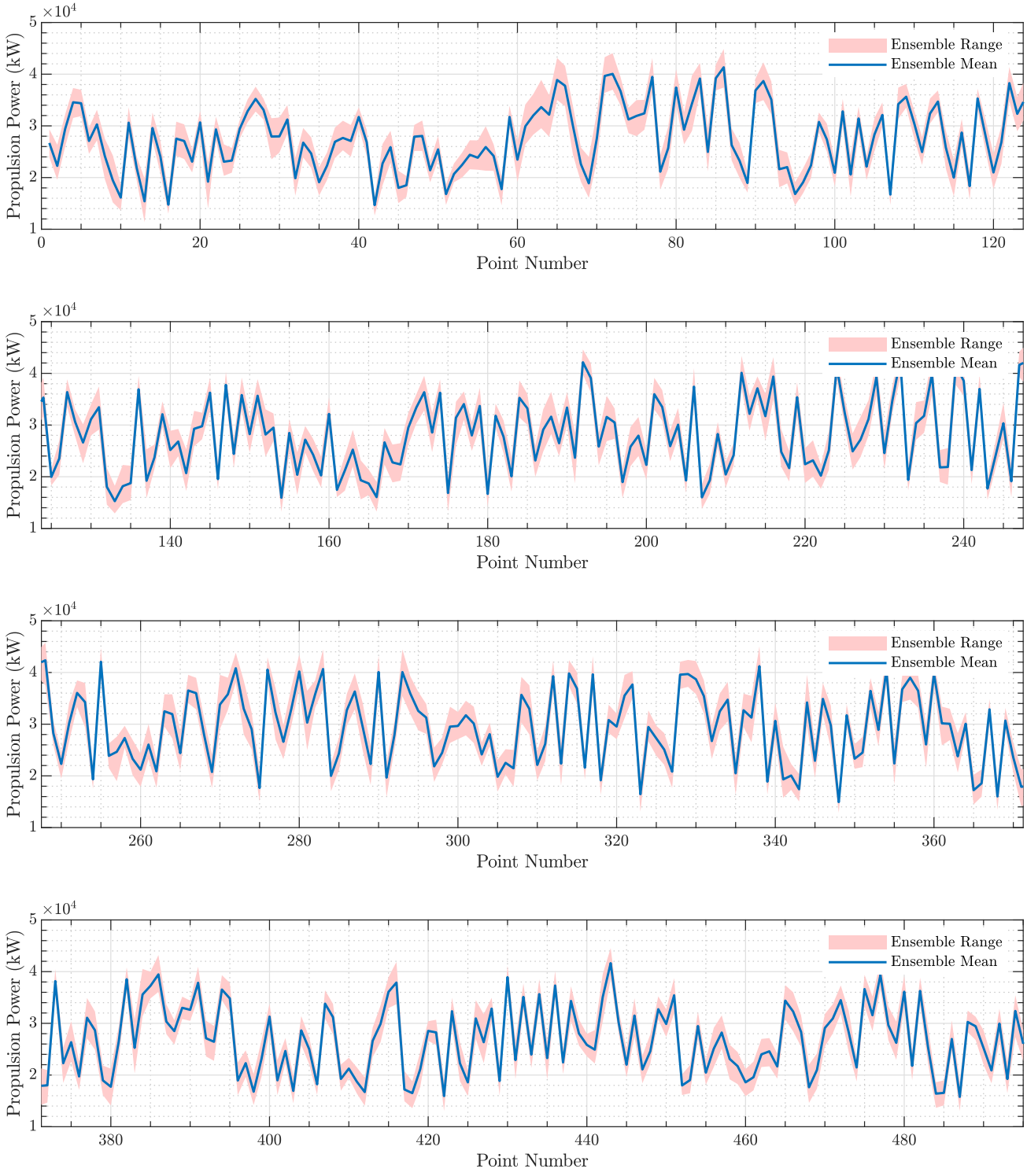

Figure 13. The ensemble ship propulsion power outputs of the created FFNN models for the considered route points. The solid line is the mean of each ensemble, while the shaded area around it is the ensemble range. (This figure is available in colour online).

negative skewness indicates the opposite (mean less than the median). Kurtosis provides information about the relative peakedness or flatness of each point distribution compared to the normal distribution. Positive kurtosis in the table implies heavier tails and a sharper peak than the normal distribution.

Figure 17 shows the probability histogram plot of the ship propulsion power ensemble members of the considered points to identify similarities or differences in the distributions. By comparing the histograms, it is possible to observe how the power requirements change across different route points. The total area under the

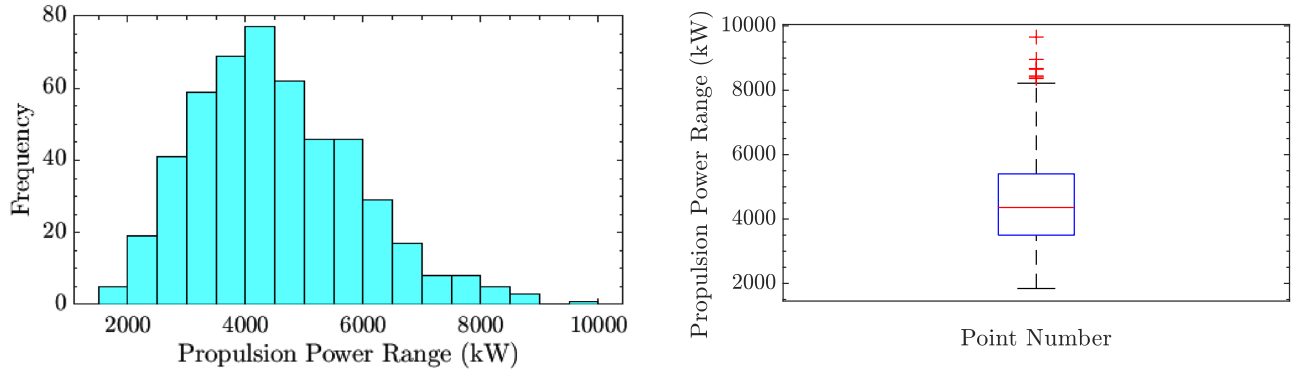

Figure 14. Histogram and boxplot of the uncertainty range of the ship propulsion power outputs of the considered route points. (This figure is available in colour online).

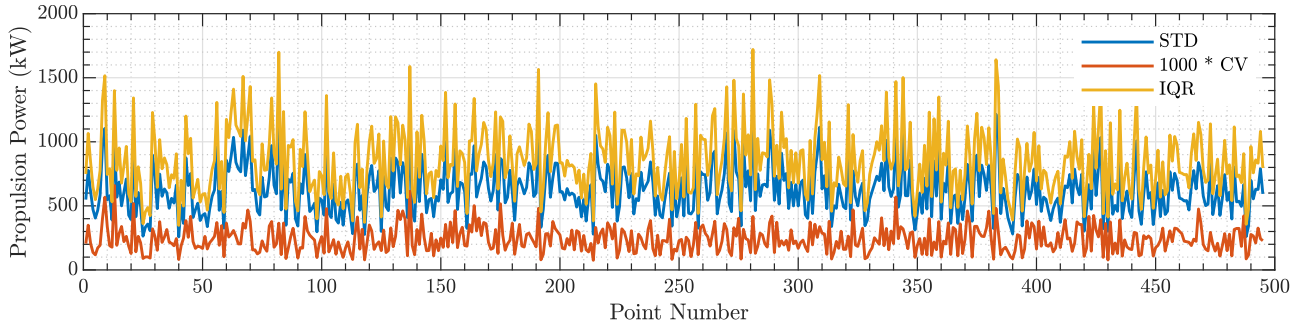

Figure 15. STD, CV, and IQR of the considered route points ship propulsion ensemble members. (This figure is available in colour online).

histogram is equal to one, indicating that it's normalized to represent probabilities. Peaks in the histogram indicate regions where the data is more concentrated. As it is clear in this figure, the x-axis represents the power output, while the y-axis represents the probability. The scales on the x-axis vary, indicating different ranges of power outputs for each route point. In general, the distribution of data is different and this difference is not too much. The peaks of the histograms indicate the most probable power outputs at each route point. The spread of the histograms shows the variability in power outputs. A wider spread indicates more variability, while a narrower spread indicates more consistency in the power output.

The box plot of the ensemble members of the ship propulsion power outputs of the considered route points is illustrated in Figure 18. This plot gives information about the central tendency and spread of the data. The box represents the IQR range, which is the range between the Q1 and the Q3. The length of

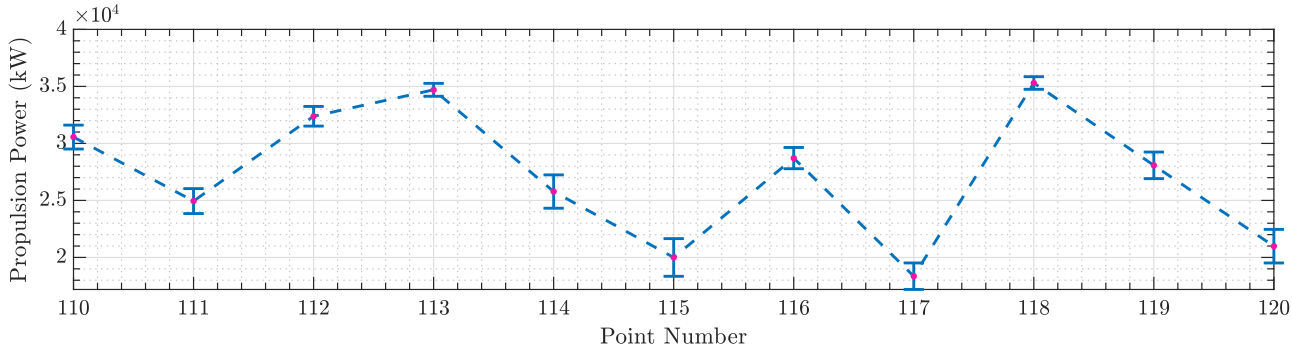

Figure 16. 95% confidence interval around the mean of the ship propulsion power outputs for some points of the considered route. (This figure is available in colour online).

Table 9. The ensemble members' central tendency, spread, and distribution measures of the ship propulsion power outputs for the considered route points.

Measure	Point 9	Point 67	Point 82	Point 137	Point 191	Point 281	Point 309	Point 341	Point 344	Point 383
Mean (kW)	19459.81	29955.84	34311.96	19218.22	23667.79	30300.83	32956.70	19318.38	34201.67	25259.46
Median (kW)	19449.57	30034.39	34319.86	19109.13	23664.92	30294.10	32981.11	19229.83	34184.03	25241.25
Range (kW)	7939.36	7654.66	8675.79	8218.85	8367.36	9652.34	7539.31	8654.82	7843.62	8958.78
First quartile (Q1) (kW)	18699.36	29250.80	33480.81	18352.02	22898.88	29434.79	32210.39	18536.01	33451.52	24426.96
Third quartile (Q3) (kW)	20215.01	30761.27	35179.94	19939.61	24463.82	31155.39	33727.56	25.67	34952.91	26067.28
Interquartile range (IQR) (kW)	1515.66	1510.47	1699.13	1587.59	1564.94	1720.60	1517.17	1469.66	1501.40	1640.32
Variance (kW^2)	1219566.36	1191847.81	1567409.39	1394063.82	1295418.12	1600279.24	1240732.14	1209641.95	1199233.33	1476674.64
Standard deviation (kW)	1104.34	1091.72	1251.96	1180.70	1138.16	1265.02	1113.88	1099.84	1095.10	1215.19
Coefficient of variation (%)	5.68	3.64	3.65	6.14	4.81	4.17	3.38	5.69	3.20	4.81
Skewness	0.05	−0.45	−0.06	0.60	−0.05	0.03	−0.10	0.44	0.08	0.10
Kurtosis	2.98	3.14	2.89	3.33	2.91	2.89	2.91	3.20	2.89	2.93

the box indicates the spread of the middle 50% of the data. A longer box indicates a larger IQR, which implies that the middle 50% of the data points are more spread out or dispersed. A larger spread indicates greater variability, while a smaller spread suggests less variability. The plot shows clear variations in the central tendency (median), dispersion (interquartile range), and outliers for each point. Points like 137, 191, 309, and 344 exhibit wider distributions, reflecting more variability in power outputs at these locations. Points 9, 67, and 341 show tighter distributions with fewer outliers, indicating more consistent power outputs. Overall, the data suggest that while some route points experience more variability in propulsion power, others are more stable, with fewer deviations among ensemble members.

Figure 19 shows the violin plot of the ensemble members of the ship propulsion power outputs versus the overall ensemble members' mean for the considered route points. The violin plot of Point 1 and Point 10 is drawn separately to show more details. A violin plot combines aspects of a box plot and a kernel density plot which is useful for visualizing the distribution and summary statistics of a data set. This figure includes

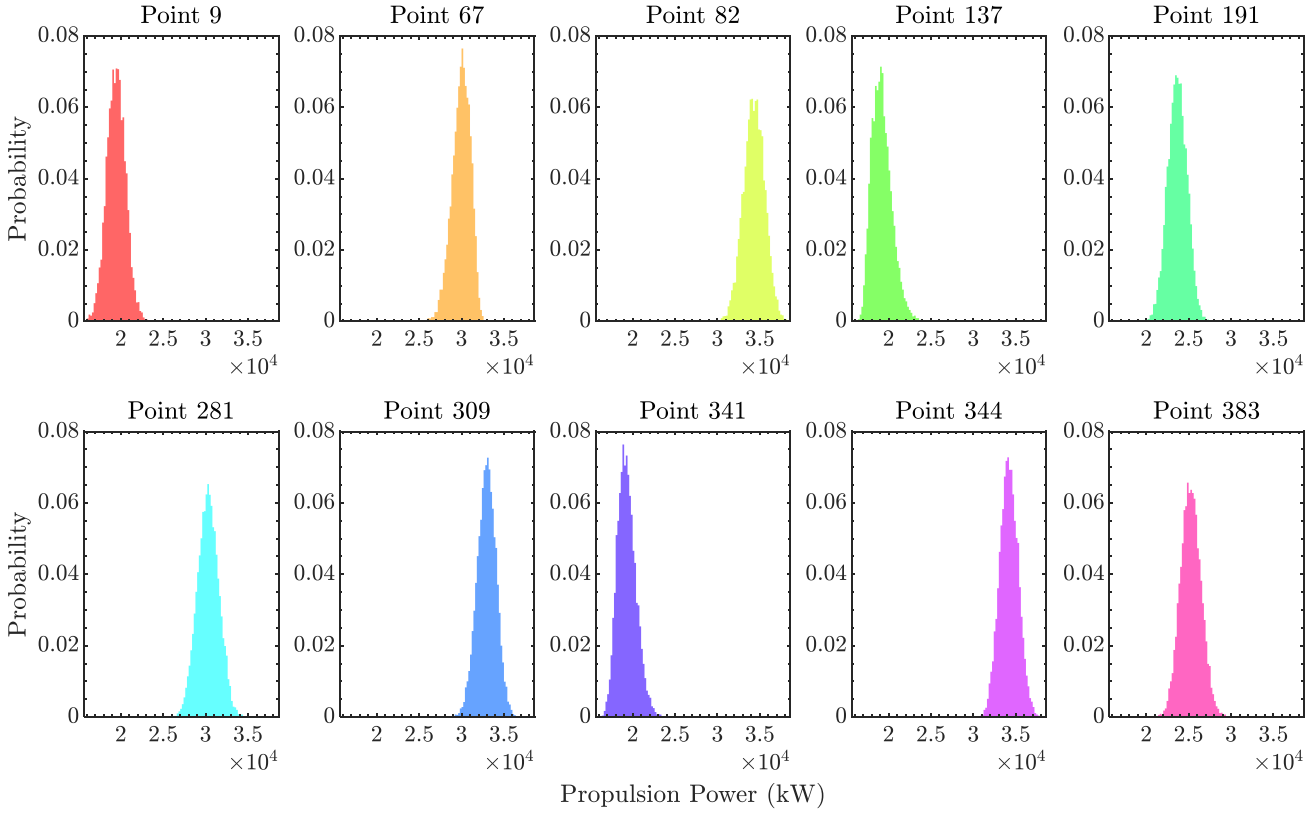

Figure 17. The probability histogram plot of the ensemble members of the ship propulsion power outputs for the considered route points. (This figure is available in colour online).

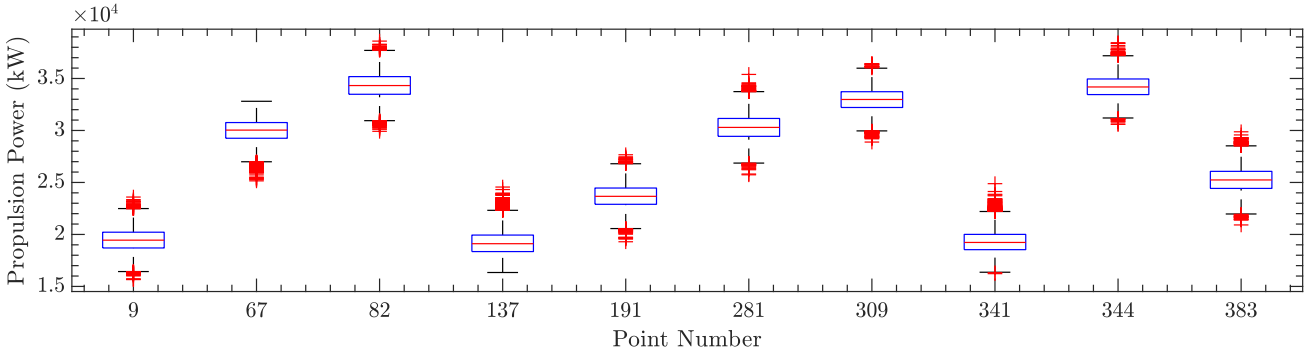

Figure 18. The box plot of the ensemble members of the ship propulsion power outputs for the considered route points. (This figure is available in colour online).

a box diagram that represents the IQR. Moreover, there is a kernel density estimation (KDE) on each side of the box plot which the right side corresponds to each point and the left side corresponds to the overall mean of all route points. The violin plot reveals asymmetries and variabilities across different route points. For example, at Points 9 and 67, the distributions are compact and have lower densities at both extremes. This suggests a relatively consistent propulsion power across ensemble members in comparison with the overall mean. However, at Points 137, 191, and 344, the violins show broader, more spread-out distributions, indicating a higher variability in propulsion power for these points. This suggests that these route points experience more diverse conditions affecting the ship's propulsion requirements. The distribution shapes provide further insights into the central tendencies and the spread of the data. Some violins exhibit long tails, such as Point 137, which suggests the presence of outliers or extreme values in the ensemble member outputs. Some points, such as 309, show more symmetrical and narrower distributions, implying that the propulsion power values are tightly clustered around the mean.

The developed strategy contributes to ship operational efficiency by providing a reliable and data-driven framework for assessing the influence of marine weather condition uncertainties on propulsion power requirements. While the model is not designed for real-time

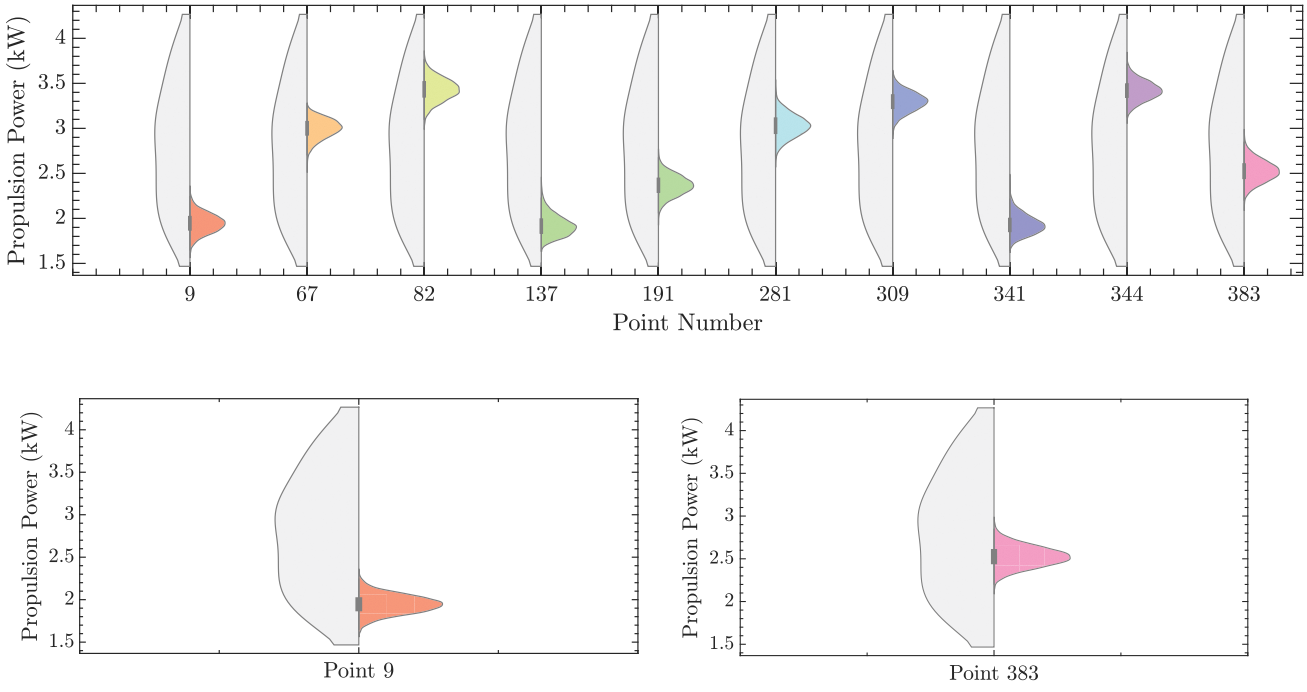

Figure 19. The violin plot of the ensemble members of the ship propulsion power outputs versus the overall ensemble members' mean for the considered route points. (This figure is available in colour online).

control, its primary function lies in enhancing strategic decision-making by offering insights into how variable environmental conditions can affect ship performance. By employing ensemble weather datasets and a trained ANN structure, the model enables a probabilistic estimation of propulsion power demands under a wide range of possible weather scenarios. This capability allows ship operators and voyage planners to better understand the risks and variability associated with weather conditions, which supports more robust operational planning, such as selecting optimal engine loads, adjusting ship speed, or modifying routes in advance. Ultimately, this proactive use of uncertainty-informed predictions can minimize unnecessary fuel consumption, prevent inefficient engine use, and reduce greenhouse gas emissions, thereby contributing to the broader goals of sustainable and cost-effective maritime transportation.

6. Conclusion

Accurate and timely weather information is crucial for safe and fuel-efficient ship navigation. In general, the weather is chaotic meaning that minor variations in its initial state can result in vastly divergent weather patterns in the coming days. This study provided valuable insights into how variations in weather factors such as wind speed and wave height impact the ship's propulsion power of a cruise ship as a case study when faced with different weather scenarios along the route. The complex relationships between weather conditions and the ship's propulsion power are ascribed using the FFNN for different weather clusters obtained by applying the SOM network. The results showed that the used FFNN can map these complex relationships with high accuracy for the studied case. Different distinct cases of weather parameters were explored to do uncertainty analysis. The created FFNN model for each cluster, when fed with ensemble weather condition data, allows for the estimation of propulsion power uncertainties using a range of statistical measures. The findings showed that power uncertainties have a significant impact on the ship's propulsion system, particularly with longer forecasting horizons. This highlights the importance of weather uncertainties in ship operations and fuel efficiency. For future studies, investigating the effects of different numerical weather models, such as global circulation models (GCMs) and regional climate models (RCMs), on the ship power performance uncertainties is suggested. Comparing the outputs of these models and assessing their reliability in predicting weather conditions relevant to ship operations can give valuable insights into the strengths and weaknesses of different modeling approaches. Exploring the propagation of uncertainties from weather models to fuel consumption estimations utilizing probabilistic methods, such as Monte Carlo simulations, is another suggestion to quantify uncertainties in fuel consumption predictions under varying weather scenarios. Analyzing the implications of these uncertainties on ship operational costs and environmental impacts is also essential. The impact of weather uncertainties on ship speed and its optimization can be assessed by developing models that integrate weather forecasts with ship hydrodynamics to predict variations in speed under different weather conditions. Probabilistic weather models can be incorporated into route planning frameworks to identify optimal paths that minimize fuel consumption, maximize safety, and adhere to scheduling constraints. Future studies could focus on developing and implementing adaptive control strategies to mitigate weather uncertainties in ship fuel consumption. These strategies would leverage real-time weather data and predictive models to dynamically adjust propulsion systems, trim, and routing decisions. Additionally, future research could explore the efficacy of model predictive control and reinforcement learning techniques in autonomously optimizing ship operations under uncertain weather conditions.

Acknowledgments

The authors express their appreciation to the reviewers for their thorough assessment and helpful feedback, which undoubtedly enhanced the paper's quality. **Kumars Mahmoodi:** Resources; Software; Data curation; Investigation; Methodology; Visualization; Formal analysis; Validation; Conceptualization; Programming; Writing – original draft; Editing. **Jari Böling:** Methodology; Resources; Software; Writing – original draft; Editing; Fund acquisition. **Abolhassan Razminia:** Methodology; Writing – original draft; Editing. **Roberto Vettor:** Methodology; Writing – original draft; Editing, NAPA API.

Author contributions

CRediT: **Kumars Mahmoodi:** Conceptualization, Data curation, Formal analysis, Investigation, Methodology, Resources, Software, Validation, Visualization, Writing – original draft, Writing – review & editing; **Jari Böling:** Data curation, Funding acquisition, Investigation, Methodology, Project administration, Writing – original draft; **Abolhassan Razminia:** Investigation, Methodology, Writing – original draft, Writing – review & editing; **Roberto Vettor:** Methodology, Writing – original draft, Writing – review & editing.

Disclosure statement

No potential conflict of interest was reported by the author(s).

Funding

This research is supported by the Business Finland project INDECS with grant number 7682/31/2022.

Ethical Approval

This paper is the author's original work and has not been previously published elsewhere.

Declaration of generative AI and AI-assisted technologies in the writing process

During the preparation of this work, the authors used ChatGPT and Microsoft Copilot to refine the language and improve clarity. After using this tool, the authors reviewed and edited the content as needed and take full responsibility for the content of the publication.

Data availability statement

The study's supporting data can be accessed by contacting the corresponding author upon request.

ORCID

Kumars Mahmoodi http://orcid.org/0000-0002-9374-5970

References

Assani N, Matić P, Kaštelan N, Čavka IR. 2023. A review of artificial neural networks applications in maritime industry. IEEE Access. 11:139823–139848. doi: 10.1109/ACCESS.2023.3341690

Bondarev A, Greiner A. 2025. Non-smooth climate change and emergent novel equilibria in an environmental-economic system. Commun Nonlinear Sci Numer Simul. 145:108686. doi: 10.1016/j.cnsns.2025.108686

Deutscher Wetterdienst. 2024. Deutscher Wetterdienst (DWD). [accessed 2024 September 20]. https://www.dwd.de.

Dickson T, Farr H, Sear D, Blake JIR. 2019. Uncertainty in marine weather routing. Appl Ocean Res. 88:138–146. doi: 10.1016/j.apor.2019.04.008

El-shenawy A, El-Hady MA, Saleh AI, Rabie AH, Takieldeen A, Shawky MA. 2025. Problem optimization of ray tracing through the crystalline lens of the eye with an artificial neural network and grey wolf optimizer. Commun Nonlinear Sci Numer Simul. 145:108733. doi: 10.1016/j.cnsns.2025.108733

Esmailian E, Steen S, Koushan K. 2022. Ship design for real sea states under uncertainty. Ocean Eng. 266:113127. doi: 10.1016/j.oceaneng.2022.113127

Glorot X, Bengio Y. 2010. Understanding the difficulty of training deep feedforward neural networks. In: Teh YW, Titterington M, editors, Proceedings of the Thirteenth International Conference on Artificial Intelligence and Statistics; Chia Laguna Resort, Sardinia, Italy: PMLR. p. 249–256. https://proceedings.mlr.press/v9/glorot10a.html.

Hummel HI, van der Mei R, Bhulai S. 2024. A survey on machine learning in ship radiated noise. Ocean Eng. 298:117252. doi: 10.1016/j.oceaneng.2024.117252

Imran MMH, Jamaludin S, Mohamad Ayob AF. 2024. A critical review of machine learning algorithms in maritime, offshore, and oil & gas corrosion research: A comprehensive analysis of ann and rf models. Ocean Eng. 295:116796. doi: 10.1016/j.oceaneng.2024.116796

Isaksen L, Bonavita M, Buizza R, Fisher M, Haseler J, Leutbecher M, Raynaud L. 2010. Ensemble of data assimilations at ecmwf. https://www.ecmwf.int/node/10125.

Kohonen T. 2001. Self-Organizing maps. Berlin Heidelberg: Springer. doi: 10.1007/978-3-642-56927-2.

Ksciuk J, Kuhlemann S, Tierney K, Koberstein A. 2023. Uncertainty in maritime ship routing and scheduling: A literature review. Eur J Oper Res. 308(2):499–524. doi: 10.1016/j.ejor.2022.08.006

Kuroda M, Sugimoto Y. 2022. Evaluation of ship performance in terms of shipping route and weather condition. Ocean Eng. 254:111335. doi: 10.1016/j.oceaneng.2022.111335

Lagemann B, Lagouvardou S, Lindstad E, Fagerholt K, Psaraftis HN, Erikstad SO. 2023. Optimal ship lifetime fuel and power system selection under uncertainty. Transp Res D Transp Environ. 119:103748. doi: 10.1016/j.trd.2023.103748

Li M, Xie C, Li X, Karoonsoontawong A, Ge YE. 2022. Robust liner ship routing and scheduling schemes under uncertain weather and ocean conditions. Transp Res C Emerg Technol. 137:103593. doi: 10.1016/j.trc.2022.103593

Liu X, Yuen KF. 2025. A systematic review on artificial intelligence applications in seaports – a network analysis approach. Expert Syst Appl. 289:128309. doi: 10.1016/j.eswa.2025.128309

Luo X, Yan R, Wang S. 2023. Comparison of deterministic and ensemble weather forecasts on ship sailing speed optimization. Transp Res D Transp Environ. 121:103801. doi: 10.1016/j.trd.2023.103801

Luo X, Zhang M, Han Y, Yan R, Wang S. 2025. Ship fuel consumption prediction based on transfer learning: models and applications. Eng Appl Artif Intell. 141:109769. doi: 10.1016/j.engappai.2024.109769

Mahmoodi K, Ghassemi H, Nowruzi H. 2018. Obtaining mathematical functions of the propeller thrust and torque coefficients fluctuations at non-uniform wake flow including geometry effects. Mech Ind. 19(2):205. doi: 10.1051/meca/2018017

Mahmoodi K, Ghassemi H, Nowruzi H, Shora MM. 2019a. Prediction of the hydrodynamic performance and cavitation volume of the marine propeller using gene expression programming. Sh Offshore Struct. 14(7):723–736. doi: 10.1080/17445302.2018.1557589

Mahmoodi K, Ghassemi H, Razminia A. 2019b. Temporal and spatial characteristics of wave energy in the persian gulf based on the era5 reanalysis dataset. Energy. 187:115991. doi: 10.1016/j.energy.2019.115991

Mahmoodi K, Ghassemi H, Razminia A. 2020. Wind energy potential assessment in the persian gulf: A spatial and temporal analysis. Ocean Eng. 216:107674. doi: 10.1016/j.oceaneng.2020.107674

Mahmoodi K, Ketabdari MJ, Vaghefi M. 2021. Proposing a new local density estimation outlier detection algorithm: an empirical case study on flow pattern experiments. Pattern Anal Appl. 24(4):1859–1872. doi: 10.1007/s10044-021-01019-2

Mahmoodi K, Nepomuceno E, Razminia A. 2022. Wave excitation force forecasting using neural networks. Energy. 247:123322. doi: 10.1016/j.energy.2022.123322

Mahmoodi K, Nowruzi H. 2022. Extreme wave height detection based on the meteorological data, using hybrid nofelm method. Sh Offshore Struct. 17(11):2520–2530. doi: 10.1080/17445302.2021.2005357

Mason J, Larkin A, Gallego-Schmid A. 2023. Mitigating stochastic uncertainty from weather routing for ships with wind propulsion. Ocean Eng. 281:114674. doi: 10.1016/j.oceaneng.2023.114674

Mittendorf M, Nielsen UD, Bingham HB, Liu S. 2022. Towards the uncertainty quantification of semi-empirical formulas applied to the added resistance of ships in waves of arbitrary heading. Ocean Eng. 251:111040. doi: 10.1016/j.oceaneng.2022.111040

NAPA. 2023. NAPA Voyage System. NAPA Voyage API. https://www.napa.fi/.

Nocedal J, Wright SJ. 2006. Numerical Optimization. volume 2 of *Numerical Mathematics and Scientific Computation*. 2 ed. New York, NY: Springer. doi: 10.1007/978-0-387-40065-5

Open-Meteo. 2024. Open-Meteo: Free Weather API. [accessed: 2024 September 20]. https://open-meteo.com.

Pereira D. 2024. Wind rose. MATLAB Central File Exchange. [accessed 2024 August 8]. https://www.mathworks.com/matlabcentral/fileexchange/47248-wind-rose.

Portillo Juan N, Negro Valdecantos V. 2022. Review of the application of artificial neural networks in ocean engineering. Ocean Eng. 259:111947. doi: 10.1016/j.oceaneng.2022.111947

Sui C, de Vos P, Hopman H, Visser K, Stapersma D, Ding Y. 2022. Effects of adverse sea conditions on propulsion and manoeuvring performance of low-powered ocean-going cargo ship. Ocean Eng. 254:111348. doi: 10.1016/j.oceaneng.2022.111348

Szlapczynski R, Szlapczynska J, Vettor R. 2023. Ship weather routing featuring w-moea/d and uncertainty handling. Appl Soft Comput. 138:110142. doi: 10.1016/j.asoc.2023.110142

Taskar B, Andersen P. 2020. Benefit of speed reduction for ships in different weather conditions. Transp Res D Transp Environ. 85:102337. doi: 10.1016/j.trd.2020.102337

The MathWorks, Inc.. 2024. Matlab – mathworks. [accessed 2024 November 18]. https://www.mathworks.com/.

Vaghefi M, Mahmoodi K, Setayeshi S, Akbari M. 2020. Application of artificial neural networks to predict flow velocity in a 180 sharp bend with and without a spur dike. Soft Comput. 24(12):8805–8821. doi: 10.1007/s00500-019-04413-5

Vettor R, Bergamini G, Guedes Soares C. 2021. A comprehensive approach to account for weather uncertainties in ship route optimization. J Mar Sci Eng. 9(12):1434. doi: 10.3390/jmse9121434

Vettor R, Soares CG. 2022. Reflecting the uncertainties of ensemble weather forecasts on the predictions of ship fuel consumption. Ocean Eng. 250:111009. doi: 10.1016/j.oceaneng.2022.111009

Wang M, Wang Y, Cui E, Fu X. 2023. A novel multi-ship collision probability estimation method considering data-driven quantification of trajectory uncertainty. Ocean Eng. 272:113825. doi: 10.1016/j.oceaneng.2023.113825

Wu Y, Sun Z, Zhao N. 2025. Resonance dynamics in multilayer neural networks subjected to electromagnetic induction. Commun Nonlinear Sci Numer Simul. 143:108575. doi: 10.1016/j.cnsns.2024.108575

Zhang Y, Zhang S, Dinavahi V. 2025. A survey of machine learning applications in advanced transportation systems: trends, techniques, and future directions. eTransportation. 24:100417. doi: 10.1016/j.etran.2025.100417

Zheng Y, Yang F, Duan J, Kurths J. 2021. Quantifying model uncertainty for the observed non-gaussian data by the hellinger distance. Commun Nonlinear Sci Numer Simul. 96:105720. doi: 10.1016/j.cnsns.2021.105720